PAPER

Check for updates

Degradation of bisphenol A during heat-activated peroxodisulfate treatment: kinetics, mechanism, and transformation products

Chunyu Wang, [ID] [a] Juan Yan,[a] Jia Yuan,[a] Ling Zhang,[a] Wei Qian,[b] Guochen Bian,[b] Yunhong Song,[a] Xu Gao [ID] *[a] and Han Mao*[c]

In this study, we systematically investigated the degradation kinetics, mechanism, and transformation products of bisphenol A (BPA) in a heat-activated peroxodisulfate (heat/PDS) system. The pseudo-first-order rate constants (k_{obs}) values of BPA increased with initial PDS dosage (0–1.0 mM), temperature (50–65 °C), and solution pH (4.0–10.0). The presence of natural organic mater (NOM), chloride ion (Cl$^-$), and bicarbonate ion (HCO$_3^-$) manifested inhibiting influence on the degradation of BPA during reaction, while nitrate (NO$_3^-$) was insignificant impact. According to radical scavenging experiments, the main oxidizing species were both hydroxyl radical (HO$^\bullet$) and sulfate radical (SO$_4^{\bullet-}$), but the HO$^\bullet$ played an important role. Transformation products were concentrated by solid phase extraction and identified by liquid chromatography high-resolution mass spectrometer (LC-HRMS). A total of fifteen transformation products derived from hydroxylation, demethylation, C–C bond cleavage, and dimerization reaction were identified. Further combining the quantum chemical calculation, the transformation pathways of BPA in the heat/PDS system were proposed. Toxicity analysis shows most of transformation products had less toxicity than that of BPA, indicating that oxidation of BPA by heat/PDS system was a detoxification process. These results illustrated that heat-activated PDS oxidation could be an efficient method to remove BPA from contaminated water.

1. Introduction

Endocrine disrupting compounds (EDCs) refer to exogenous substances capable of stimulating or suppressing endogenous hormone reactions, thereby disrupting the reproductive and developmental processes in living organisms.[1–3] Among the prevalent EDCs, bisphenol A (2,2-bis(4-hydroxyphenyl)propane, BPA) is widely used as an intermediate in the production of many consumer products, including electronic equipment, polycarbonate (PC) plastics, sports safety equipment, and epoxy resins.[4,5] BPA is a synthetic organic compound with the chemical formula $C_{15}H_{16}O_2$ and a molecular weight of 228.29 g mol^{-1}.[6] Its structure consists of two phenolic rings linked by an isopropylidene bridge, forming 4,4′-isopropylidene diphenol. The speciation of BPA (pK_{a1} = 9.6, pK_{a2} = 10.2) to monobasic BPA and dibasic BPA at pH 9. The global annual production of BPA reached 3.9 million tons in 2006, and was projected to increase by approximately 30% by 2020.[7,8] With the extensive use of these products, BPA is frequently detected in surface water, wastewater, and groundwater at concentrations typically ranging from a few ng L^{-1} to hundreds of µg L^{-1}.[6,7,9] In sediments and landfill leachates, concentrations can even reach up to mg L^{-1}.[2] Critically, BPA and its derivatives can accumulate in the food chain of humans and animals, leading to persistent chronic toxicity.[10] Consequently, developing effective technologies to degrade BPA in contaminated surface water and groundwater is urgent.

In recent years, advanced oxidation processes (AOPs), characterized by generating highly reactive species *via* oxidants activation (*i.e.*, ozone, hydrogen peroxide (H$_2$O$_2$), peroxymonosulfate (PMS), and peroxydisulfate (PDS)), have been widely explored for degrading refractory organic compounds in water.[11–14] Among these, the *in situ* generated sulfate radical (SO$_4^{\bullet-}$) from activation of PMS/PDS has attracted significant attention.[15,16] Compared to hydroxyl radical (HO$^\bullet$, 10^{-3} µs), SO$_4^{\bullet-}$ possesses a longer half-life (30–40 µs), and it exhibits stronger selectivity with a high redox potential (E^0 = 2.5–3.1 V).[17,18] Compared to H$_2$O$_2$ (the HO$^\bullet$ precursor), the SO$_4^{\bullet-}$ precursors (PMS/PDS) are increasingly applied as alternatives to HO$^\bullet$-based AOPs for removing refractory organic contaminants in waste waters and subsurface environments.[19,20] In general, PDS alone with most organic compounds at a low reactivity.[18]

[a]*Chaohu Regional Collaborative Technology Service Center for Rural Revitalization of Anhui Province, School of Biological and Environmental Engineering, Chaohu University, Hefei, 238000, China. E-mail: gaoxun@chu.edu.cn; Tel: +86-0551-82369184*

[b]*Anhui Green Energy Technology Institute Co., Hefei, 238088, China*

[c]*South China Institute of Environment Sciences, Ministry of Ecology and Environment, Guangdong, 510655, China. E-mail: maohan@scies.org*

However, the generated $SO_4^{\bullet-}/HO^{\bullet}$ from PDS activation *via* varieties of methods, including heating, ultraviolet (UV) irradiation, heterogeneous catalytic, and transition metals.[21–23]

Among these activation methods, heat activation of PDS has attracted increasing attention due to environmental friendliness, convenient operation, and lack of secondary pollution (*i.e.*, metal ions dissolution from various catalyst).[24–26] Heat activation typically involves injecting hot water or steam into the contaminated area, or applying electrical resistance heating, to activate the PDS for *in situ* remediation of the contaminated soil.[25] Although previous studies have exported that BPA can be effectively degraded by $SO_4^{\bullet-}$-based AOPs, including zero valent iron, ferrous iron, carbon-based materials, and microwave activated PDS.[27–30] However, the reactive sites of BPA molecule react with free radicals in heat/PDS system were largely unknown. Several studies only focus on the decomposition rate or degradation efficiency of BPA, while were difficult to further identify the molecule structures of transformation products from BPA in these processes.[16] Quantum chemical calculation is effectively supplement to the experimental results and can be used to examine the reaction mechanism.[31–33] While researchers have studied oxidation reactions of contaminants with $SO_4^{\bullet-}$ or $HO^{\bullet}$, insufficient mechanisms and kinetic data are available on the degradation of BPA by these radicals.[20,34] Furthermore, investigations on the water matrices affect the degradation of BPA in heat/PDS system are still limited.

In this work, the degradation of BPA in heat/PDS system was systematically investigated. The main purposes of this study were to (1) investigate the degradation kinetic of BPA in the heat/PDS system; (2) explore the effects of water matrix (including nitrate (NO_3^-), chloride ion (Cl^-), bicarbonate ion (HCO_3^-), and natural organic matter (NOM)) on the degradation of BPA; (3) identify the contributions of reactive species during the reactions; (4) identify the transformation products and degradation pathways of BPA in the heat/PDS system according to quantum chemical calculations and mass spectrometer analysis; (5) evaluate the ecotoxicity of BPA and its transformation products during heat/PDS system. This work aims to provide useful information for evaluating the feasibility of degradation of BPA in contaminated water using $SO_4^{\bullet-}$-based AOPs.

2. Materials and methods

2.1. Materials and reagents

All chemicals and reagents used in this study were of analytical grade, and were provided in Text S1 of the SI. Ultra-pure water (18.25 MΩ cm^{-1}) used in all prepared solution.

2.2. Experimental procedures

Batch experiments were conducted in a water bath (SN-HWS-8F, Sunne, China) thermostatically at 60 ± 0.5 °C. 50 mL reaction solutions consisted of 1 mM PDS, 40 μM BPA, and 10 mM phosphate buffer (for its negligible effect on the reactions) at pH 7.0 ± 0.1. Sulfuric acid and sodium hydroxide were applied to adjust the initial pH of the reaction solutions to 4.0, 5.5, 7.0, 8.5,

and 10.0. Control experiments were also performed in the absence of PDS under the above same condition. Methanol (MeOH), isopropanol (IPA), and *tert*-butanol (TBA) were added to the reaction solution to investigate the main reactive species. NO_3^-, Cl^-, HCO_3^-, and NOM (0–10 mg L^{-1}, was obtained from the Suwannee river (#1R101F)) were added into the reaction solution to investigate the influence of water matrices on BPA degradation during heat/PDS treatment. At the pre-set time points, 0.8 mL samples were withdrawn, immediately quenched by 10 μL of 2 M sodium sulfite, and stored in a liquid phase vial for subsequent analysis. All the experiments were carried out at least twice.

To further identify the transformation products of BPA, 200 mL reaction solution consisted of 40 μM BPA, 1 mM PDS, and 10 mM phosphate buffer was allowed to reaction for 60 min under 60 ± 0.5 °C. Then, the reaction solution was chilled and rapidly enriched *via* solid phase extraction (SPE) using balanced-reverse-polymer (BRP) cartridges (120 mg/6 cm^3). More details of SPE procedures are given in Text S2 of the SI.

2.3. Analytical methods

Concentration of BPA was analyzed by a high-performance liquid chromatography (HPLC, LC-20, Shimadzu, Japan) coupled with an C18 column (5 μm, 250 mm × 4.6 mm, Agilent, USA). The flow rate was 1.0 mL min^{-1}, and the injection volume was 10 μL. The mobile phase was consisted of 70% MeOH (with 0.1% formic acid) and 30% water (with 0.1% formic acid). The detection wavelength and reaction time of BPA were 280 nm and 3.550 min, respectively.

BPA and its transformation products were characterized using high-resolution mass spectrometer (HRMS) comprised of a HPLC coupled with a Q-Exactive mass spectrometer (Thermo Fisher Scientific, USA). Separation was accomplished using an ZORBAX SB-C18 column (5 μm, 100 mm × 2.1 mm, Agilent, USA). Detailed analytic parameters of HRMS were obtained in Text S3 of the SI.

2.4. Theoretical calculations

Density functional theory (DFT) calculations were performed using Gaussian 16 at the M062X/6-31+G(d,p) level. The M062X functional was selected, as it is well-suited for modeling $SO_4^{\bullet-}/HO^{\bullet}$ reactions and thermodynamic calculations for main-group elements.[35] Optimized geometries at stable points exhibited positive vibrational frequencies, while transition states possessed a single imaginary frequency.[20] Intrinsic reaction coordinate (IRC) calculations verified connectivity between transition states, reactants, and products.[32] To model aqueous environments, solvent effects were incorporated using the SMD solvation model with water. Based on optimized structures, Multiwfn 3.7 analyzed localized Fukui function distributions and frontier molecular orbitals (FMOs) to predict radical attack sites. FMOs were visualized using VMD 1.9.3.

2.5. Toxicity assessment

The toxicity of BPA and its transformation products to aquatic organisms was assessed by Ecological Structure–Activity

Relationship Model (E.C.O.S.A.R.) software (version 1.11).[36–38] In terms of acute toxicity, 96 h 50% lethal concentration (LC$_{50}$) for fish, 48 h LC$_{50}$ for daphnia, and 96 h 50% effective concentration (EC$_{50}$) for green algae. In addition, the ChV toxicity of BPA and its transformation products to fish, daphnia, and green algae was also investigated.

3. Results and discussion

3.1. Degradation kinetics of BPA in heat/PDS system

The degradation kinetics of BPA in heat/PDS system was explored. As shown in Fig. 1(a), no degradation of BPA was observed in the control experiments without PDS at 120 min, suggesting that BPA degradation efficiency was unlikely affected by the volatilization of BPA. However, 41.1% of BPA was degraded by 0.2 mM PDS at 60 °C within a reaction time of 120 min in the heat/PDS system, and BPA degradation efficiency increased from 41.1% to 100% with the increase of PDS dosage increased from 0.2 to 1.0 mM. The degradation data of BPA followed pseudo-first-order kinetics model. The pseudo-first-order rate constant, k_{obs}, was obtained from linear regression of ln [BPA]$_t$/[BPA]$_0$ against t at each condition (eqn (1)).

$$-\mathrm{Ln}\frac{[\mathrm{BPA}]_t}{[\mathrm{BPA}]_0} = k_{obs}t \tag{1}$$

where [BPA]$_0$ and [BPA]$_t$ are the concentrations of BPA at time 0 and t, respectively. At PDS dosage concentration of 0.2 mM, the value of k_{obs} for BPA degradation was 0.0046 min^{-1} (Fig. S1(a)). Further increasing PDS dosage concentration to 1.0 mM, the k_{obs} value was increased to 0.0290 min^{-1}. As shown in Fig. 1(b), a linear relationship can be established between the k_{obs} and PDS dosages. These results indicated that BPA can be effectively degraded in the heat/PDS system.

The influence of reaction temperature on the degradation of BPA in water was investigated. As presented in Fig. 1(c), the degradation of BPA increased with increasing reaction temperature. The value of k_{obs} increased from 0.0073 to 0.053 min^{-1} with increasing reaction temperature from 55 °C to 65 °C (Fig. S1(b)). This is due to the accelerated rate of PDS decomposition to generate some reactive species as the reaction temperature increased, which accelerated the degradation of BPA in the heat/PDS system. Note that, while the reaction temperature was elevated to 80 °C, the increase in the k_{obs} value became insignificant (Fig. S2). This result indicated that employing the heat/PDS system to treat BPA wastewater, economic applicability should be considered. In addition, Fig. 1(d) shows the degradation of BPA in acidic condition was significantly higher than that in alkaline condition. As seen in Fig. S1(c), the k_{obs} value reached 0.0046, 0.029, 0.0249, 0.0363, and 0.0564 min^{-1} within 120 min at the solution pH of 4.0, 5.5, 7.0, 8.5, 10.0, respectively, indicating that the heat/PDS oxidation system has good acid-base adaptability for BPA degradation. The observed inhibition under acidic conditions (Fig. 1(d)) arises from (i) protonation of SO$_4$$^{\bullet-}$ to less reactive hydrogen sulfate radicals (HSO$_4$$^{\bullet}$), and (ii) suppression of the HO$^{\bullet}$/SO$_4$$^{\bullet-}$ interconversion pathway. This phenomenon was also observed in a prior study,[39] where the degradation efficiency of

sulfamethoxazole exhibited a significantly inhibitory effect under acidic conditions. Despite structural/chemical differences, the degradation behavior of BPA and SMX confirmed that pH primarily affects degradation efficiency by regulating the type of free radical rather than relying on compound specific structures.

3.2. Identification of reactive species

It has been reported that some reactive species (*i.e.*, HO$^{\bullet}$ and SO$_4$$^{\bullet-}$) were expected to be generated from the heat/PDS system.[24] In this study, MeOH, TBA, and IPA were used as scavengers to explore the contributions of HO$^{\bullet}$/SO$_4$$^{\bullet-}$ responsible for the degradation of BPA. In general, MeOH can rapidly react with both HO$^{\bullet}$ and SO$_4$$^{\bullet-}$ ($k_{\mathrm{MeOH,HO^{\bullet}}} = 9.7 \times 10^8$ M^{-1} s^{-1}, $k_{\mathrm{MeOH,SO_4^{\bullet-}}} = 1.1 \times 10^7$ M^{-1} s^{-1}), while TBA reacts with HO$^{\bullet}$ more quickly than SO$_4$$^{\bullet-}$ ($k_{\mathrm{TBA,HO^{\bullet}}} = 6 \times 10^8$ M^{-1} s^{-1}, $k_{\mathrm{TBA,SO_4^{\bullet-}}} = 4 \times 10^5$ M^{-1} s^{-1}).[40] As shown in Fig. 2, the degradation efficiency of BPA was decreased in the presence of MeOH and TBA. The k_{obs} value of BPA after 120 min of reaction decreased from 0.0290 min^{-1} to 0.0164 min^{-1} and 0.0134 min^{-1} when 10 mM MeOH and 10 mM TBA spiked (Fig. S3). Compared to MeOH, IPA reacts with HO$^{\bullet}$ and SO$_4$$^{\bullet-}$ at a second reaction rate constants of 1.9×10^9 and 8.2×10^7 M^{-1} s^{-1}, respectively.[40,41] It reacts considerably faster with HO$^{\bullet}$ and SO$_4$$^{\bullet-}$. The k_{obs} value of BPA after 120 min further declined to 0.0027 min^{-1} when 10 mM IPA spiked. These results demonstrated that both HO$^{\bullet}$ and SO$_4$$^{\bullet-}$ were the primary reactive species on BPA degradation in heat/PDS system, but HO$^{\bullet}$ played more important role.

3.3. Effects of anions and NOM on the degradation of BPA in heat/PDS system

Previous studies have shown that degradation of pollutants in wastewater and natural waters may be influenced by the presence of co-existing anions.[25,39] In this study, the effects of common anions, such as NO$_3$$^-$, Cl$^-$, and HCO$_3$$^-$, on the degradation of BPA were explored, and the experimental data are displayed in Fig. 3(a). As seen, no significant change was observed on BPA degradation in the presence of 5 mM NO$_3$$^-$. When the concentration of NO$_3$$^-$ increased from 5 to 50 mM, the degradation of BPA was only slightly inhibited, which is consistent with previously reported result that the reaction between SO$_4$$^{\bullet-}$ and NO$_3$$^-$ with a low second reaction rate constant of 2.1×10^0 M^{-1} s^{-1}.[42]

However, the degradation efficiency of BPA was decreased in the presence of Cl$^-$ (Fig. 3(b)). The k_{obs} value of BPA after 120 min was declined from 0.0290 to 0.0093 min^{-1} when the concentration of Cl$^-$ increased from 0 to 50 mM (Fig. S4(a)). This is due to the competition of Cl$^-$ with BPA for HO$^{\bullet}$/SO$_4$$^{\bullet-}$ to form reactive chlorine species, such as chlorine radicals (*i.e.*, Cl$^{\bullet}$ and Cl$_2$$^{\bullet-}$) and hypochlorous acid (HClO).[43] Compared with HO$^{\bullet}$/SO$_4$$^{\bullet-}$, the generated reactive chlorine species have relative lower oxidation potential which are generally less reactive towards organic compounds. Therefore, in this study, Cl$^-$ acts as HO$^{\bullet}$/SO$_4$$^{\bullet-}$ scavenger, resulting in the degradation of BPA was decreased. Similar results were also found in the degradation of BPA by heat/PDS with HCO$_3$$^-$. As shown in Fig. 3(c), the
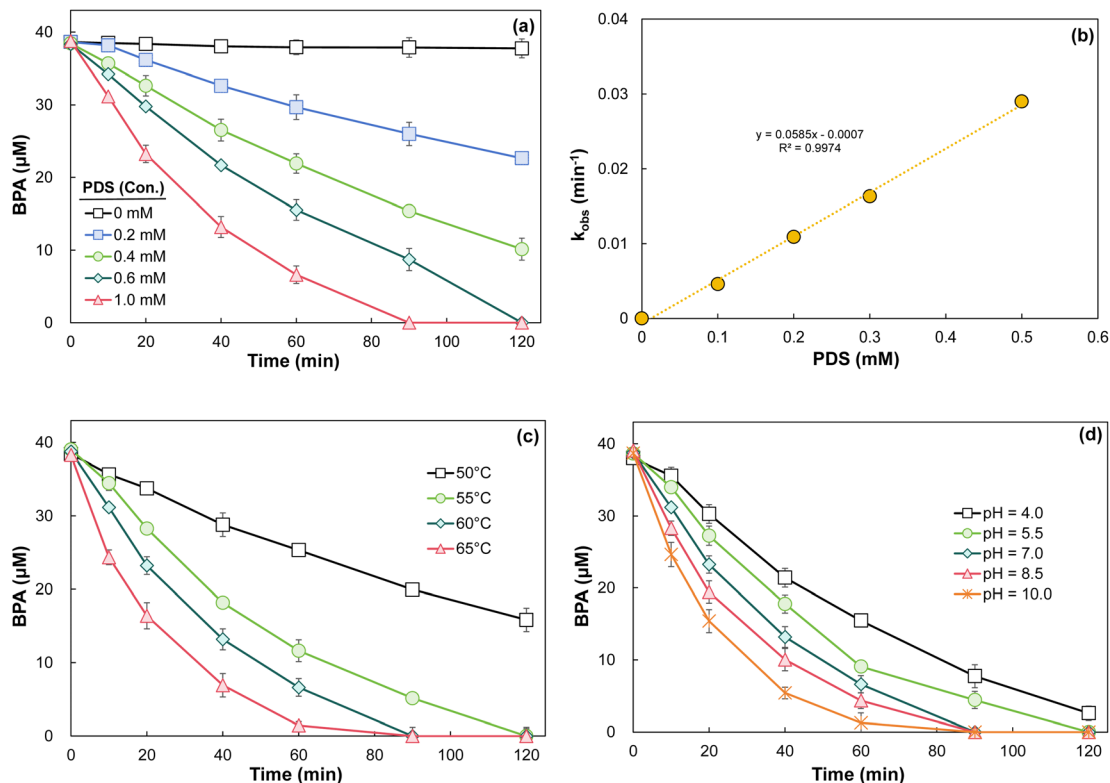
Fig. 1 Effects of (a) initial PDS dosage at 60 °C on BPA degradation in heat/PDS system. (b) Relationship between the observed pseudo-first-order rate constant (k_{obs}) of BPA degradation and PDS dosages. Effects of (c) reaction temperature and (d) solution pH on BPA degradation in heat/PDS system. Experimental conditions: $[BPA]_0 = 40$ μM, $[PDS]_0 = 1.0$ mM, pH 7.0 ± 0.1 maintained by 10.0 mM phosphate buffer.
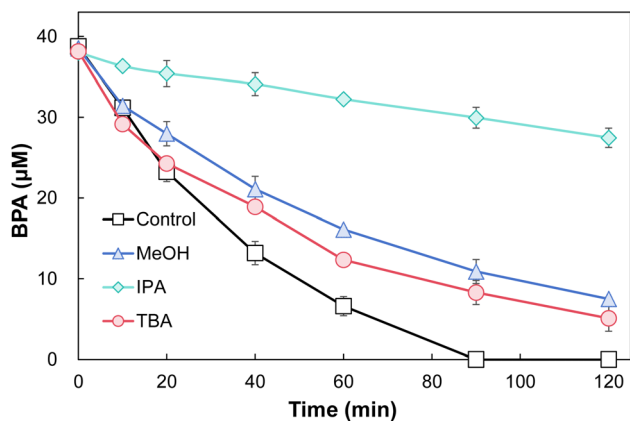

Fig. 2 Effects of MeOH, TBA, and IPA on the degradation of BPA in heat/PDS system. Experimental conditions: $[BPA]_0 = 40$ μM, $[PDS]_0 = 1.0$ mM, $[MeOH]_0 = 10$ mM, $[TBA]_0 = 10$ mM, $[IPA]_0 = 10$ mM, pH 7.0 ± 0.1 maintained by 10.0 mM phosphate buffer.

degradation efficiency of BPA in the presence of 5 mM HCO_3^- after 90 min reached 90.5% lower than that in the absence of HCO_3^-. The k_{obs} value of BPA was decreased from 0.0260 to 0.0176 min^{-1} when the concentration of HCO_3^- increased from 5 to 50 mM (Fig. S4(b)). The reason may be attributed to the reaction between HCO_3^- and $HO^•/SO_4^{•-}$ to generate relative weaker oxidation radical, such as bicarbonate radical ($HCO_3^•$).[44]

In addition, NOM widely present in natural water and have a strong effect on organic compounds degradation in heat/PDS system.[45] In this study, the influence of different NOM concentrations (0–10 mg L^{-1}) on BPA degradation was explored, the experimental data were displayed in Fig. 3(d) and S3(c). As seen, a significant inhibition for the degradation of BPA in heat/PDS system with NOM concentrations of 2, 4, 6, and 10 mg L^{-1}, with the corresponding k_{obs} value of 0.0243, 0.0188, 0.0150, and 0.0108 min^{-1}, respectively (Fig. S4(c)). This is because NOM was susceptible to be attacked by reactive species to generate small-molecular organic fractions, which may compete with the parent pollutants and thus decrease their degradation efficiency. Note that, the reaction between NOM and $HO^•$ was greater than that between NOM with $SO_4^{•-}$.[43] Therefore, the reactive species formed in the heat/PDS system led to the attenuation of BPA degradation efficiency in the presence of NOM.

3.4. Products identification and degradation pathways

Combined with DFT calculation and degradation products detection through HRMS, the potential degradation pathway of BPA in heat/PDS system was investigated. As shown in Fig. 4(a), the molecular structure of BPA molecule with atomic numbering. Of which, the highest occupied molecular orbital (HOMO) of BPA molecule mainly localizes on the benzene ring and hydroxyl (–OH) functional groups (Fig. 4(b)), indicating
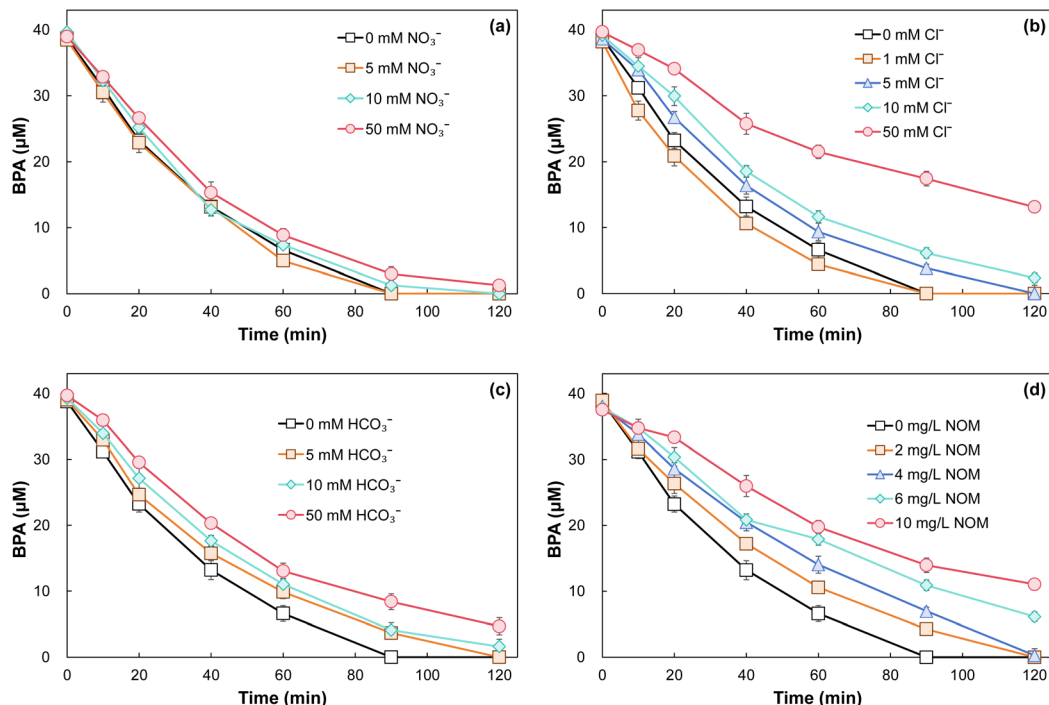
Fig. 3 Effects of (a) NO_3^-, (b) Cl^-, (c) HCO_3^-, and (d) NOM on the degradation of BPA in heat/PDS system. Experimental conditions: $[BPA]_0 = 40$ μM, $[PDS]_0 = 1.0$ mM, $[NO_3^-]_0 = 0$–50 mM, $[Cl^-]_0 = 0$–50 mM, $[HCO_3^-]_0 = 0$–50 mM, $[NOM]_0 = 0$–10 mg L^{-1}, pH 7.0 ± 0.1 maintained by 10.0 mM phosphate buffer.

these sites more susceptible to electrophilic interactions.[32,46] Note that, these electron-rich sites on the BPA molecule were more likely to react with $HO^{\bullet}/SO_4^{\bullet-}$. To assess the vulnerable sites of BPA, the corresponding values of Fukui index were utilized in this part. As shown in Fig. 4(c), the two carbon atoms

C2 and C12 within the benzene ring exhibit the highest f^0 value, implying that these reaction positions more susceptible to free radical attack. In addition, the two sites C6 and C16 possessed a relative higher f^0 value.

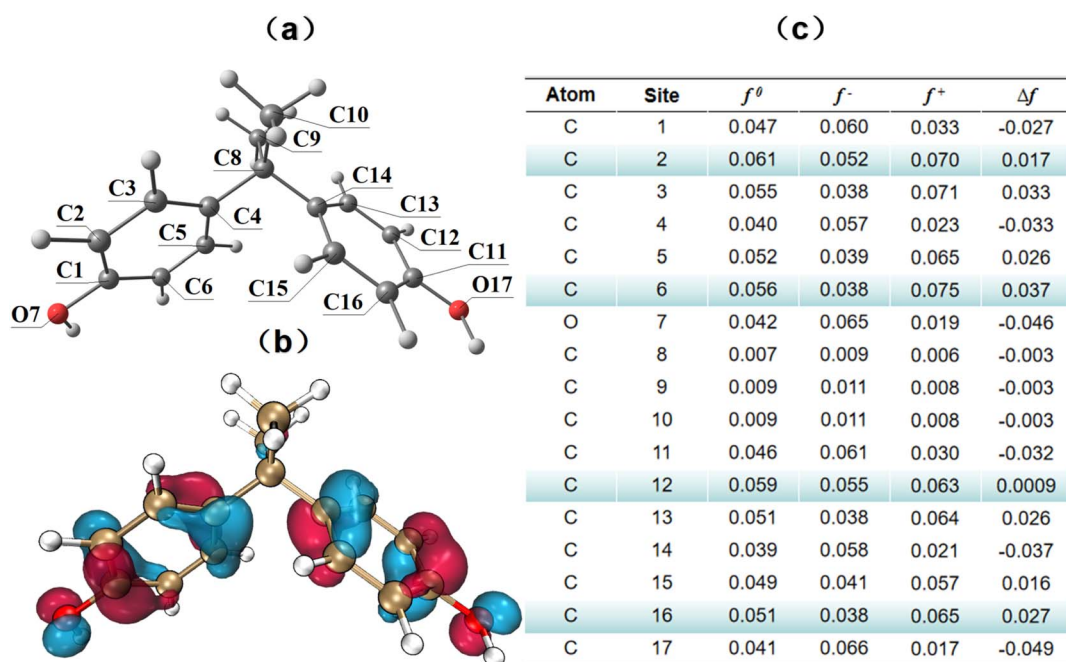| Atom	Site	f^0	f^-	f^+	Δf
C	1	0.047	0.060	0.033	-0.027
C	2	0.061	0.052	0.070	0.017
C	3	0.055	0.038	0.071	0.033
C	4	0.040	0.057	0.023	-0.033
C	5	0.052	0.039	0.065	0.026
C	6	0.056	0.038	0.075	0.037
O	7	0.042	0.065	0.019	-0.046
C	8	0.007	0.009	0.006	-0.003
C	9	0.009	0.011	0.008	-0.003
C	10	0.009	0.011	0.008	-0.003
C	11	0.046	0.061	0.030	-0.032
C	12	0.059	0.055	0.063	0.0009
C	13	0.051	0.038	0.064	0.026
C	14	0.039	0.058	0.021	-0.037
C	15	0.049	0.041	0.057	0.016
C	16	0.051	0.038	0.065	0.027
C	17	0.041	0.066	0.017	-0.049

Fig. 4 (a) Molecular structure, (b) HOMO (the two-color representation for positive/negative wavefunction phases), and (c) Fukui index of BPA molecule.
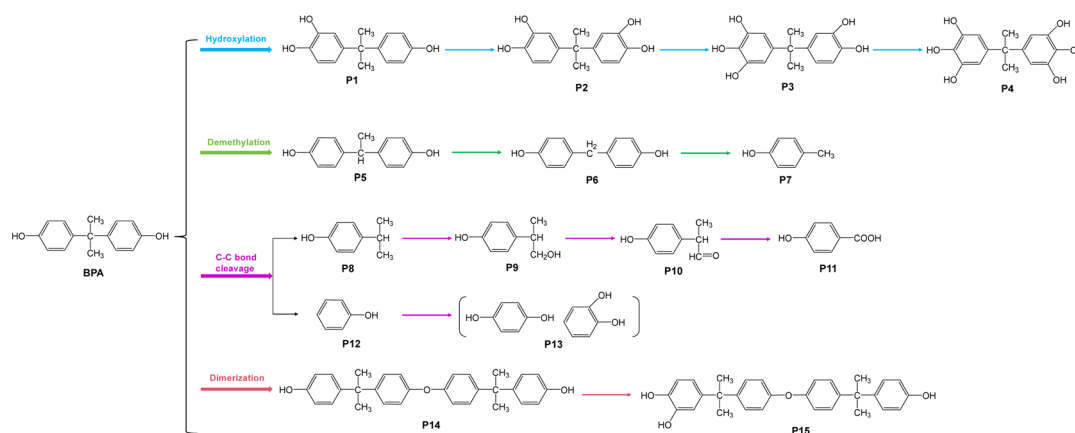
Fig. 5 Possible degradation pathway of BPA in heat/PDS system.

During heat/PDS system, the transformation products of BPA were identified by HRMS. The corresponding mass charge ratio (m/z) and spectrum of BPA and its transformation products were provided in Table S1. Through the obtained transformation products and DFT calculation, four possible degradation pathways for BPA were proposed in Fig. 5, including hydroxylation, demethylation, C–C bond cleavage, and dimerization. In pathway 1, the C2 atom of BPA was susceptible to radical attack because it has a high reactivity ($f^0 = 0.061$), thus BPA was hydroxylated by HO$^•$ to generate P1 (m/z 227.12741). Similar results were also obtained from Fig. 6. As seen, HO$^•$ addition to the C2 atom of BPA with a lowest ΔE value (4.34 kcal mol^{-1}), indicating that the C2 site more susceptible to HO$^•$ addition. This process involves several steps as follow. Firstly, HO$^•$ attacked the C2 atom of BPA
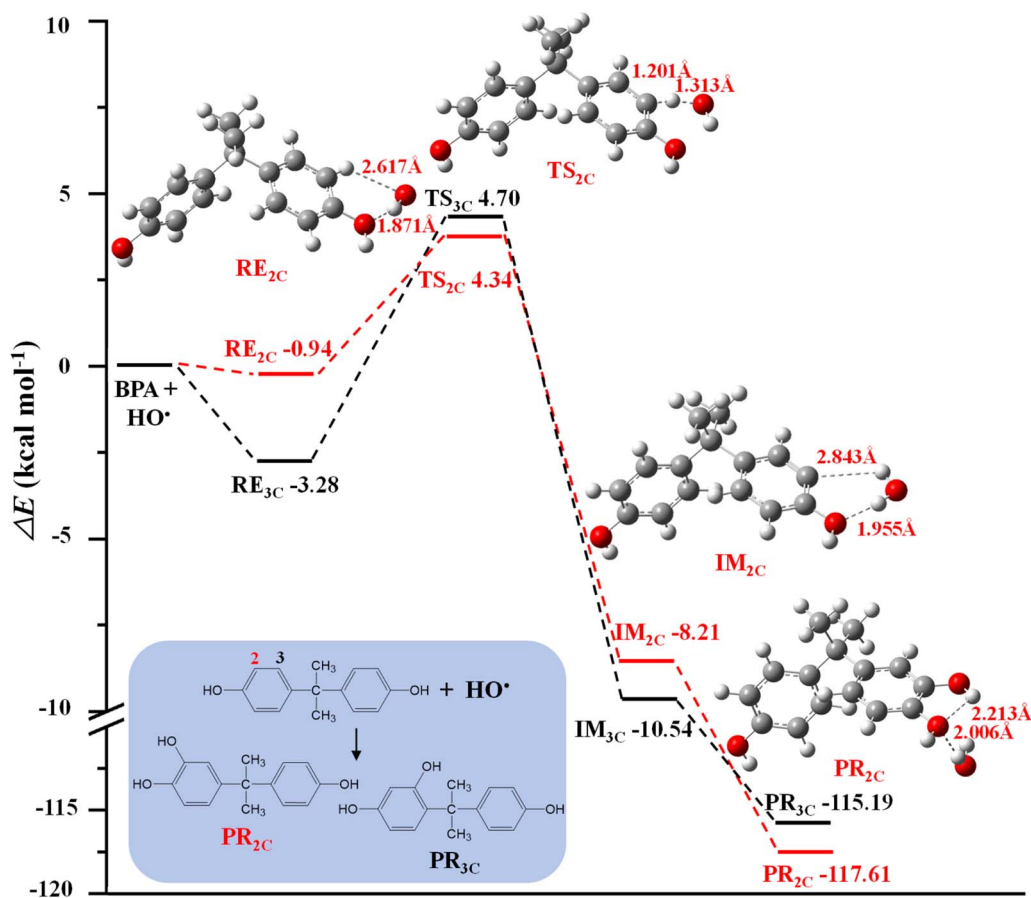

Fig. 6 Calculation of the ΔE value for HO$^•$ addition reactions at different C sites of BPA molecule.
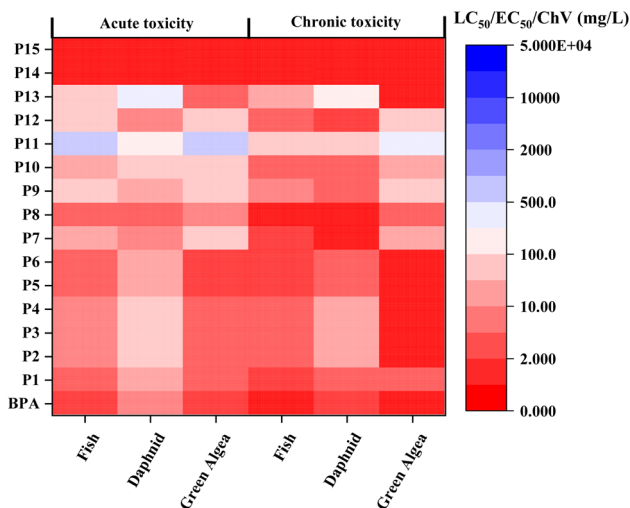
Fig. 7 Acute and chronic toxicity of BPA and its transformation products to fish, daphnid, and green algae *via* E.C.O.S.A.R. software (version 1.11).

with the initial C–H bond length at 2.617 Å. However, this value gradually decreased to 1.201 Å in the transition state (TS) 2C. Secondly, a H atom left from the plane of the BPA molecule, and the length value of bond C–H was increased to 2.843 Å, leading to the formation of intermediate (IM) 2C. Finally, the produced IM 2C reacted with another HO$^{\bullet}$ to form a product (PR) 2C. In addition to the C2 site, HO$^{\bullet}$ also attack the C3 site generating a hydroxyl adduct IM 3C with a ΔE value of 4.70 kcal mol^{-1} (Fig. S5). However, this value was lower than that of C2 site, indicating that the C2 site of BPA was the reaction site for HO$^{\bullet}$ addition. Therefore, BPA was first attacked by HO$^{\bullet}$ to generate P1. Then, hydroxylation of P1 occurred to form P2 (m/z 258.91504). The generated P2 was further hydroxylated by HO$^{\bullet}$ due to the relatively high f^{0} value of C6 (0.056), resulting in the production of P3 (m/z 277.09781). Further hydroxylation of P3 occurred to produce P4 (m/z 290.90201).

In pathway 2, demethylation of BPA molecule by HO$^{\bullet}$/SO$_4^{\bullet-}$ attack leads to the formation of P5 (m/z 213.01425). Further demethylation of P5 occurred to produce P6 (m/z 199.90761). The cleavage of the C–C bond leads to the generation of P7 (m/z 109.02868). In pathway 3, the cleavage of the C–C bond of BPA molecule leads to the production of P8 (m/z 135.04716) and P12 (m/z 95.06091). On the one hand, P8 is oxidized by HO$^{\bullet}$ to produce P9 (m/z 153.09103), which was then transformed into P10 (m/z 149.02335) and P11 (m/z 137.02303) by HO$^{\bullet}$/SO$_4^{\bullet-}$ attack. On the other hand, BPA underwent a cleavage of the C–C bond to produce P12, which was transformed into P13 (m/z 111.05555) because the attack of HO$^{\bullet}$ on the benzene ring. In pathway4, BPA is first attacked by free radicals to produce a phenoxy radical. Then, the two phenoxy radical are coupled to produce P14 (m/z 439.30029). Subsequently, hydroxylation of P14 occurred to generate P15 (m/z 455.27890).

3.5. Toxic assessment of BPA in heat/PDS system

To assess the ecological safety of the heat/PDS system, the acute and chronic toxicity of the BPA and its transformation products

was conducted by quantitative structure activity relationship (QSAR) model analysis with E.C.O.S.A.R. software. In general, all the organic compounds were given in the unit of mg L^{-1}, which fall into four toxicity grades, *e.g.*, very toxic (<1.0), toxic (1.0–10.0), harmful (10.0–100.0), and not harmful (>100.0). The acute and chronic toxicity evaluation of the BPA and its transformation products were illustrated in Fig. 7(b). As seen, the acute toxicity of BPA to fish, daphnid, and green algae was in the toxic grade, while the chronic toxicity of BPA to fish and green algae was in the very toxic grade. However, P1–P13 of the transformation products were less harmful than BPA, indicating that the aquatic toxicity of BPA after heat/PDS treatment was generally reduced along the degradation pathways (hydroxylation, demethylation, and C–C bond cleavage). In addition, the acute and chronic toxicity of dimerization products (P14 and P15) to fish, daphnid, and green algae were in the very toxic grade, which also proves that the trend of increased toxicity of dimerization reaction. Therefore, additional attention should be paid to these toxic dimerization products produced in the heat/PDS system.

4. Conclusion

This study demonstrated that BPA can be effectively degraded by heat/PDS system. The k_{obs} value of BPA was increased with the increasing initial PDS dosage (0–1.0 mM) and reaction temperature (50–65 °C), which was primarily attributed to the enhanced formation of reactive species. BPA is more likely to be degraded by heat/PDS system under alkaline conditions (solution pH 10.0) than that under acidic conditions (solution pH 4.0). According to quenching experiments, both HO$^{\bullet}$ and SO$_4^{\bullet-}$ were confirmed to be the main reactive species involved in BPA degradation, but HO$^{\bullet}$ played an important role. NOM, Cl$^-$, and HCO$_3^-$ acts as scavengers of HO$^{\bullet}$/SO$_4^{\bullet-}$ and decreases the degradation of BPA, while NO$_3^-$ poses an insignificant influence on BPA degradation. Based on the DFT calculations, BPA is more likely to be oxidized by HO$^{\bullet}$/SO$_4^{\bullet-}$, four possible degradation pathways were proposed, including hydroxylation, demethylation, C–C bond cleavage, and dimerization reactions. In addition, E.C.O.S.A.R. results showed that the toxicity of BPA was decreased after heat/PDS treatment. These findings provide a new insight for BPA degradation into the reaction mechanism of heat activated PDS system.

Author contributions

Chunyu Wang: investigation, formal analysis, data curation, writing – original draft, funding acquisition. Juan Yan: writing – review & editing. Jia Yuan: writing – review & editing, funding acquisition. Ling Zhang: writing – review & editing, funding acquisition. Wei Qian: writing – review & editing. Guochen Bian: writing – review & editing. Yunhong Song: writing – review & editing, funding acquisition. Xu Gao: writing – review & editing, funding acquisition, conceptualization, supervision. Han Mao: writing – review & editing, conceptualization, supervision.

Conflicts of interest

The authors declare that they have no known competing financial interests or personal relationships that could have appeared to influence the work reported in this paper.

Data availability

The data that support the findings of this study are available on reasonable request from the corresponding author [Xu Gao, gaoxun@chu.edu.cn].

The SI includes chemicals, SPE procedures, instrumental setup of HRMS, and MS data of samples. See DOI: https://doi.org/10.1039/d5ra04707b.

References

1 K. Czarny-Krzymińska, B. Krawczyk and D. Szczukocki, Bisphenol A and its substitutes in the aquatic environment: occurrence and toxicity assessment, *Chemosphere*, 2023, **315**, 137763.

2 Y. Q. Huang, C. K. C. Wong, J. S. Zheng, H. Bouwman, R. Barra, B. Wahlström, *et al.*, Bisphenol A (BPA) in China: a review of sources, environmental levels, and potential human health impacts, *Environ. Int.*, 2012, **42**, 91–99.

3 W. H. Qiu, H. Y. Zhan, J. Q. Hu, T. Zhang, H. Xu, M. H. Wong, *et al.*, The occurrence, potential toxity, and toxicity mechanism of bisphenol S, a substitute of bisphenol A: a critical review of recent progress, *Ecotoxicol. Environ. Saf.*, 2019, **173**, 192–202.

4 L. M. Ma, P. Xue, Z. G. Gao, C. R. Xu and P. Li, Mineralized degradation of bisphenol A by novel photoenzyme-metal catalyst FCAP@Ag$_3$PO$_4$/Lac-Pd beads, *J. Environ. Manage.*, 2025, **388**, 126042.

5 J. R. Xiong, S. Y. Hu, Z. X. Xu, C. Q. Li, Z. H. Li, S. Y. Li, *et al.*, Different paths, same destination: Bisphenol A and its substitute induce the conjugative transfer of antibiotic resistance genes, *Chemosphere*, 2024, **368**, 143625.

6 H. Wang, Z. Tang, Z. H. Liu, F. Zeng, J. Zhang and Z. Dang, Occurrence, spatial distribution, and main source identification of ten bisphenol analogues in the dry season of the Pearl River, South China, *Environ. Sci. Pollut. Res.*, 2022, **29**(18), 27352–27365.

7 R. P. Huang, Z. H. Liu, S. F. Yuan, H. Yin, Z. Dang and P. X. Wu, Worldwide human daily intakes of bisphenol A (BPA) estimated from global urinary concentration data (2000-2016) and its risk analysis, *Environ. Pollut.*, 2017, **230**, 143–152.

8 K. Pivnenko, D. Laner and T. F. Astrup, Dynamics of bisphenol A (BPA) and bisphenol S (BPS) in the European paper cycle: need for concern?, *Resour., Conserv. Recycl.*, 2018, **133**, 278–287.

9 H. D. Zhou, X. Huang, X. L. Wang and X. H. Wen, Evaluation of estrogenicity of sewage samples from Beijing, China, *Environ. Sci.*, 2009, **30**, 3590–3595.

10 R. G. Wang, T. J. Tan, H. J. Liang, Y. Huang, S. J. Dong, P. L. Wang, *et al.*, Occurrence and distribution of bisphenol compounds in different categories of animal feeds used in China, *Emerging Contam.*, 2021, **7**, 179–186.

11 D. Wang, K. Luo, H. L. Tian, H. J. Cheng, S. Giannakis, Y. Song, *et al.*, Transforming plain LaMnO$_3$ perovskite into a powerful ozonation catalyst: elucidating the mechanisms of simultaneous A and B sites modulation for enhanced toluene degradation, *Environ. Sci. Technol.*, 2024, **58**(27), 12167–12178.

12 R. C. Zhang, Y. K. Yang, C. H. Huang, N. Li, H. Liu, L. Zhao, *et al.*, UV/H$_2$O$_2$ and UV/PDS treatment of trimethoprim and sulfamethoxazole in synthetic human urine: transformation products and toxicity, *Environ. Sci. Technol.*, 2016, **50**(5), 2573–2583.

13 T. Zhang, Y. C. Wen, Z. L. Pan, Y. Kuwahara, K. Mori, H. Yamashita, *et al.*, Overcoming acidic H$_2$O$_2$/Fe(II/III) redox-induced low H$_2$O$_2$ utilization efficiency by carbon quantum dots fenton-like catalysis, *Environ. Sci. Technol.*, 2022, **56**(4), 2617–2625.

14 Y. F. Zhen, S. S. Zhu, Z. Q. Sun, Y. Tian, Z. Li, C. Yang, *et al.*, Identifying the persistent free radicals (PFRs) formed as crucial metastable intermediates during peroxymonosulfate (PMS) activation by N-doped carbonaceous materials, *Environ. Sci. Technol.*, 2021, **55**(13), 9293–9304.

15 G. P. Anipsitakis, D. D. Dionysiou and M. A. Gonzalez, Cobalt-mediated activation of peroxymonosulfate and sulfate radical attack on phenolic compounds. Implications of chloride ions, *Environ. Sci. Technol.*, 2006, **40**(3), 1000–1007.

16 J. L. Wang and S. Z. Wang, Activation of persulfate (PS) and peroxymonosulfate (PMS) and application for the degradation of emerging contaminants, *Chem. Eng. J.*, 2018, **334**, 1502–1517.

17 G. V. Buxton, C. L. Greenstock, W. P. Helman and A. B. Ross, Critical review of rate constants for reactions of hydrated electrons, hydrogen atoms and hydroxyl radicals ($^\bullet$OH/$^\bullet$O$^-$) in aqueous solution, *J. Phys. Chem. Ref. Data*, 1988, **17**(2), 513–886.

18 S. Padmaja, Z. B. Alfassi, P. Neta and R. E. Huie, Rate constants for reactions of SO$_4^{\bullet-}$ radicals in acetonitrile, *J. Chem. Kinet.*, 1993, **25**(3), 193–198.

19 S. K. Guo, X. Y. Wang, W. Chen, J. Y. Xu and H. M. Jiang, Enhancing degradation of sulfapyridine by magnetic Fe$_2$O$_3$-CoFe$_2$O$_4$@NC prepared through a facile solid phase coordination-calcination method for peroxymonosulfate activation, *Chem. Eng. J.*, 2024, **489**, 151204.

20 Q. Mei, J. F. Sun, D. N. Han, B. Wei, Z. X. An, X. Y. Wang, *et al.*, Sulfate and hydroxyl radicals-initiated degradation

reaction on phenolic contaminants in the aqueous phase: mechanisms, kinetics and toxicity assessment, *Chem. Eng. J.*, 2019, **373**, 668–676.

21 Y. W. Gao, Y. Zhu, T. Li, Z. H. Chen, Q. Jiang, Z. Y. Zhao, X. Y. Liang, *et al.*, Unraveling the high-activity origin of single-atom iron catalysts for organic pollutant oxidation via peroxymonosulfate activation, *Environ. Sci. Technol.*, 2021, **55**(12), 8318–8328.

22 T. Zeng, X. F. Tang, Z. Q. Huang, H. Chen, S. J. Jin, F. L. Dong, *et al.*, Atomically dispersed Fe-N₄ site as a conductive bridge enables efficient and stable activation of peroxymonosulfate: active site renewal, anti-oxidative capacity, and pathway alternation mechanism, *Environ. Sci. Technol.*, 2023, **57**(49), 20929–20940.

23 R. C. Zhang, P. Z. Sun, T. H. Boyer, L. Zhao and C. H. Huang, Degradation of pharmaceuticals and metabolite in synthetic human urine by UV, UV/H₂O₂, and UV/PDS, *Environ. Sci. Technol.*, 2015, **49**(5), 3056–3066.

24 L. W. Chen, X. X. Hu, T. M. Cai, Y. Yang, R. D. Zhao, C. Liu, *et al.*, Degradation of triclosan in soils by thermally activated persulfate under conditions representative of in situ chemical oxidation (ISCO), *Chem. Eng. J.*, 2019, **369**, 344–352.

25 Y. F. Ji, Y. Y. Shi, W. Dong, X. Wen, M. D. Jiang and J. Lu, Thermo-activated persulfate oxidation system for tetracycline antibiotics degradation in aqueous solution, *Chem. Eng. J.*, 2016, **298**, 225–233.

26 Y. F. Ji, Y. Y. Shi, L. Wang and J. H. Lu, Denitration and renitration processes in sulfate radical-mediated degradation of nitrobenzene, *Chem. Eng. J.*, 2017, **315**, 591–597.

27 Z. L. Li, C. T. Wu, J. Y. Yang, J. H. Guo and W. Xiong, Efficiency and mechanism of phosphoric acid modified biochar loaded nanoscale zero-valent iron activated peroxymonosulfate for the degradation of bisphenol A, *Chem. Eng. Sci.*, 2024, **295**, 120132.

28 X. X. Peng, Y. Tian, S. W. Liu and X. S. Jia, Degradation of TBBPA and BPA from aqueous solution using organo-montmorillonite supported nanoscale zero-valent iron, *Chem. Eng. J.*, 2017, **309**, 717–724.

29 R. L. Luo, Z. C. Yang, Y. C. Wang, Y. Yang, L. Y. Qi, J. W. Qi, *et al.*, Fe-loaded hollow fiber carbon microfiltration membrane and its BPA removal performance based on electro-Fenton, *J. Environ. Chem. Eng.*, 2025, **13**(2), 116098.

30 S. Li, G. Zhang, P. Wang, H. S. Zheng and Y. J. Zheng, Microwave-enhanced Mn-Fenton process for the removal of BPA in water, *Chem. Eng. J.*, 2016, **294**, 371–379.

31 P. P. Zamora, K. Bieger, A. Cuchillo, A. Tello and J. P. Muena, Theoretical determination of a reaction intermediate: Fukui function analysis, dual reactivity descriptor and activation energy, *J. Mol. Struct.*, 2021, **1227**, 129369.

32 L. Meng, J. Dong, J. Chen, L. Li, Q. Huang and J. Lu, Activation of peracetic acid by spinel FeCo₂O₄ nanoparticles for the degradation of sulfamethoxazole, *Chem. Eng. J.*, 2023, **456**, 141084.

33 P. Du, W. Liu, H. Cao, H. Zhao and C. H. Huang, Oxidation of amino acids by peracetic acid: reaction kinetics, pathways and theoretical calculations, *Water Res.: X*, 2018, **1**, 100002.

34 Q. Han, M. M. Wang, F. Y. Sun, B. P. Yu, Z. J. Dong, P. Li, *et al.*, Effectiveness and degradation pathways of bisphenol A (BPA) initiated by hydroxyl radicals and sulfate radicals in water: initial reaction sites based on DFT prediction, *Environ. Res.*, 2023, **216**, 114601.

35 L. Feng, W. W. Song, N. Oturan, M. Karbasi, E. D. van Hullebusch, G. Esposito, *et al.*, Electrochemical oxidation of naproxen in aqueous matrices: elucidating the intermediates' eco-toxicity, by assessing its degradation pathways via experimental and density functional theory (DFT) approaches, *Chem. Eng. J.*, 2023, **451**, 138483.

36 L. Wang, Y. Q. Yu, G. Q. Liu and J. H. Lu, Formation of brominated by-products during the degradation of tetrabromobisphenol S by Co²⁺/peroxymonosulfate oxidation, *J. Environ. Manage.*, 2022, **314**, 115091.

37 Z. Y. Li, X. L. Wang, F. Peng, N. Chen and G. D. Fang, Organic radicals driving polycyclic aromatic hydrocarbon polymerization with peracetic acid activation in soil, *J. Hazard. Mater.*, 2024, **475**, 134839.

38 L. N. Yin, J. Y. Wei, Y. M. Qi, Z. N. Tu, R. J. Qu, C. Yan, *et al.*, Degradation of pentachlorophenol in peroxymonosulfate/heat system: kinetics, mechanism, and theoretical calculations, *Chem. Eng. J.*, 2022, **434**, 134736.

39 Y. F. Ji, Y. Fan, K. Liu, D. Y. Kong and J. H. Lu, Thermo activated persulfate oxidation of antibiotic sulfamethoxazole and structurally related compounds, *Water Res.*, 2015, **87**, 1–9.

40 L. W. Gao, Y. Guo, J. L. Zhan, G. Yu and Y. Y. Wang, Assessment of the validity of the quenching method for evaluating the role of reactive species in pollutant abatement during the persulfate-based process, *Water Res.*, 2022, **221**, 118730.

41 Z. Liu, L. Liu, S. Q. He, Y. Chen, S. Q. Zhang, X. B. Dong, *et al.*, Quenching should be used with caution to evaluate the role of reactive oxygen species in the degradation of pollutants by electro-advanced oxidation technology, *Process Saf. Environ. Prot.*, 2025, **195**, 106823.

42 Y. F. Ji, L. Wang, M. D. Jiang, J. H. Lu, C. Ferronato and J. M. Chovelon, The role of nitrite in sulfate radical-based degradation of phenolic compounds: an unexpected nitration process relevant to groundwater remediation by in-situ chemical oxidation (ISCO), *Water Res.*, 2017, **123**, 249–257.

43 Q. Y. Li, F. Y. Fang and W. M. Chen, Effect of a high Cl⁻ concentration on the transformation of waste leachate DOM by the UV/PMS system: a mechanistic study using the Suwannee River natural organic matter (SRNOM) as a simulator of waste leachate DOM, *J. Hazard. Mater.*, 2025, **487**, 137038.

44 Y. Yang, X. L. Lu, J. Jiang, J. Ma, G. Q. Liu, Y. Cao, *et al.*, Degradation of sulfamethoxazole by UV, UV/H₂O₂ and UV/

RSC Advances

Paper

persulfate (PDS): formation of oxidation products and effect of bicarbonate, *Water Res.*, 2017, **118**, 196–207.

45 J. F. Li, W. L. Qin, B. Zhu, T. Ruan, Z. C. Hua, H. Y. Du, *et al.*, Insights into the transformation of natural organic matter during UV/peroxydisulfate treatment by FT-ICR MS and machine learning: non-negligible formation of organosulfates, *Water Res.*, 2024, **256**, 121564.

46 L. Meng, J. Y. Dong, J. Chen, J. H. Lu and Y. F. Ji, Degradation of tetracyclines by peracetic acid and UV/peracetic acid: reactive species and theoretical computations, *Chemosphere*, 2023, **320**, 137969.